Tengstrand's "3-2-1"-Sculpture and New Derivatives

Carlo H. Séquin
CS Division, University of California, Berkeley, CA, USA; sequin@berkeley.edu

Abstract

This is an analysis of the geometry of the "3-2-1"-sculpture by Tord Tengstrand, presented at the Bridges 2020 Art Exhibition. Derivative shapes are then obtained by changing some of the geometrical parameters. In one extension, the 3-fold rotational symmetry of the original sculpture is changed to values ranging from 2 to 6. In another extension, the complexity of the iterated edge-curve is enhanced to make more passes around the central void. In addition, one half of some of those derivative geometries are used as a modular building block for the more complex polyhedral frames structures based on the Platonic solids.

1. Introduction

In the Bridges 2020 Art Exhibition, Tord Tengstrand [7] presented an intriguing sculpture (Fig.1a) called "3-2-1", since it had 3 curved edges, 2 pointy vertices, but only a single, higly curved, multi-branch "face" that connects to itself across the three "loopy" edges. I don't recall whether I saw it in 2020; but recently I came across an image of it in the Bridges archives. From a single image it is difficult to understand this shape. A lively email exchange helped Tord and me to understand this shape and its topological parameters.

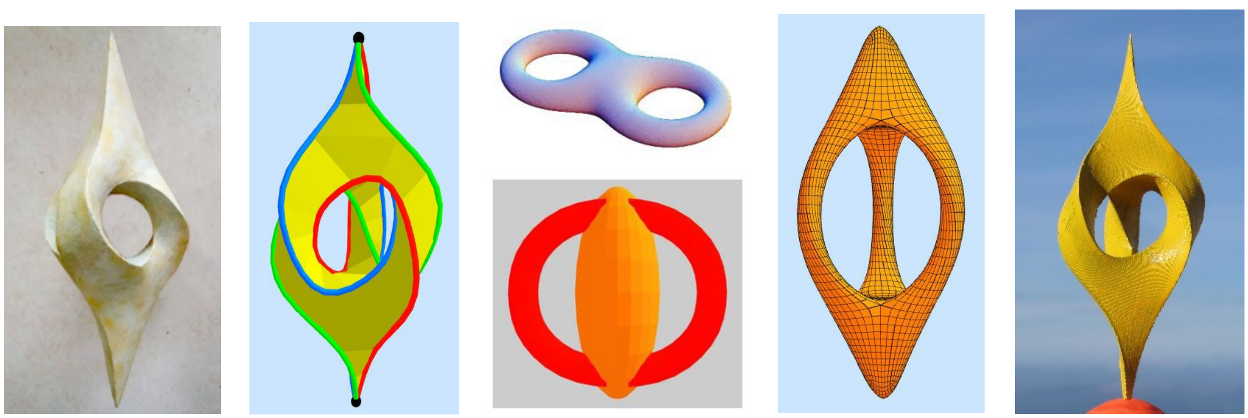

(a) (b) (c) (d) (e)

Figure 1: *: (a) Tengstrand's "3-2-1"-Sculpture. (b) CAD model showing the 2 vertices and the 3 edges; (c,d) handlebodies of genus 2. (e) 3D-print, painted yellow.*

Tord's "3-2-1"-sculpture is a handlebody of genus 2 with 3-fold rotational symmetry around an axis that passes through the two (black) vertices in Figure 1b. Even though this model seems to have three "tunnels," only two of its three solid prismatic branches need to be cut to turn it into a genus-0 object. Thus, the genus of this handlebody is 2; and it is topologically equivalent to a 2-hole torus, or to a spherical blob with two handles attached to it (Fig.1c). Embedded in a handlebody with 3-fold rotational symmetry (Fig.1d) are three identical, loopy edges with a dihedral angle of about 60 degrees (shown in red, green, and blue) that run from one vertex to the other one (Fig.1b). Each edge makes a "down-up-down" zig-zag motion that passes the central void three times. I call this a "3-pass edge."

Between neighboring edges there are three "N"-shaped ribbons (shown in yellow, orange, and magenta in Figs.2a,b & 3a), which also make 3-pass, up-down, zig-zag moves that start at one 3-way junction and end at the other one. These ribbons border one another across the three loopy edges, but they are also smoothly connected to one another in the two junction areas. The resulting topology of the resulting overall "face" is shown in Figure 3d. It can also be seen as a hollow sphere with three slits in it (Fig.3e).

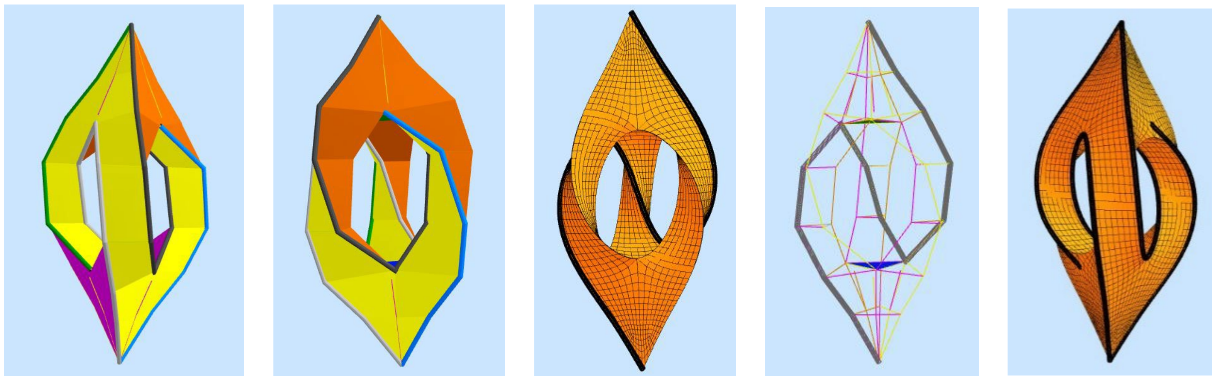

(a) (b) (c) (d) (e)

Figure 2: *The 3 edges in the "3-2-1"-Sculpture: (a,b) Front and back views of a polyhedral model with sharp edges highlighted. (c,d) A single edge on the smoothed model, and in isolation. (e) Edges segments needed to define the sharp edges around a single ribbon component.*

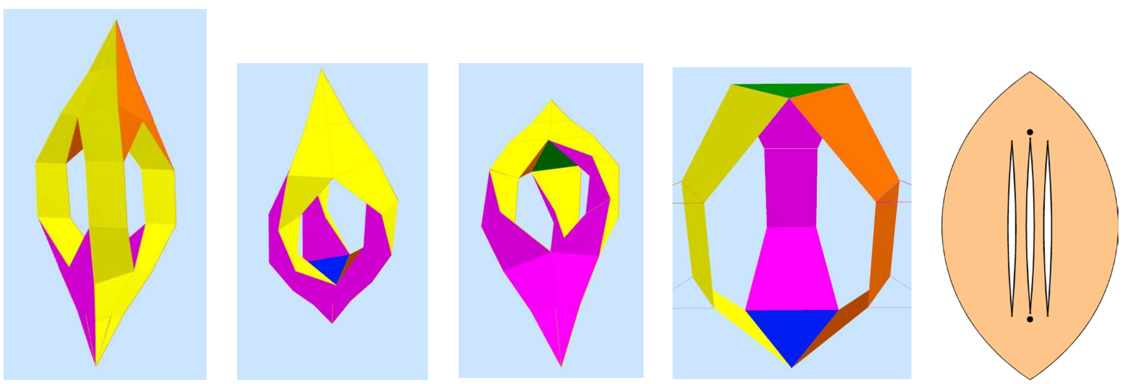

(a) (b) (c) (d) (e)

Figure 3: *The face of the "3-2-1"-sculpture: (a) The zig-zag motion of one ribbon-like component; (b,c) lower and upper 3-way junction areas; (d,e) simple topological models of the whole face.*

Modeling Issues

To make a clean CAD model of this sculpture, our home-brewed JIPCAD environment (Joint Interactive & Procedural Computer-Aided Design) [2],[3],[4] is well suited. It allows the user to specify some geometry, such as the loopy edges, in a procedural manner, e.g., as cubic B-splines. Surface facets between these edges can then be added interactively through the graphical user interface. The symmetry of these shapes can easily be exploited by defining just one loopy edge and then instantiating that edge three times with rotations of 120 degrees between them. Similarly, the D_3 symmetry of this shapes requires that only 1/6 of the overall surface must be constructed explicitly. The bottom half of the model can be obtained by flipping the top half through 180 degrees around the x-axis. This is how I created my first CAD model.

I started my design based on one edge-curve because this was a key feature in the "3-2-1"-sculpture. I modeled half of the edge-curve with a B-spline, displaying it with about 12 discrete linear segments. Then, I properly placed three copies of it and turned on "*vertex-selection*" in our CAD tool. This displays all vertices as selectable entities that can be used to define facets between them (Fig.4b). By selecting two pairs of vertices on two neighboring edge-curves I could form a small quad face. Near the two tips of the sculpture, it was easy to construct good facets; sometimes I used just a triangle (Fig.4c). In the middle of the sculpture, it is more difficult! In some places, the vertices do not line up in an obvious way. Nevertheless, I found a valid solution (Fig.4d) that forms a closed surface with no open border segments, and which resulted in a good polyhedral model (Fig.4e).

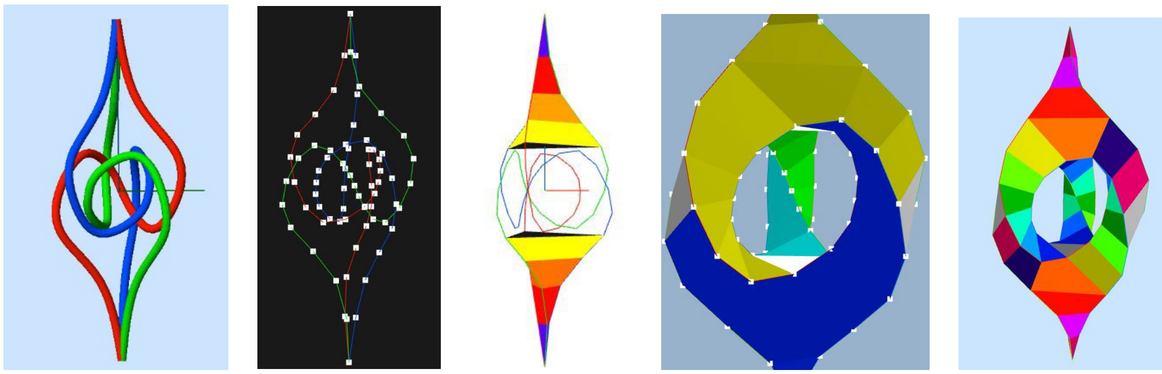

(a) (b) (c) (d) (e)

Figure 4: *Modeling based on edges: (a) Desired edge configuration. (b) Displaying selectable vertices. (c) Modeling the 2 pyramids; (d) constructing the central parts; (e) resulting polyhedral model.*

However, even if I could properly close the surface, the three resulting prismatic branches my not exhibit a nice cross-section in the shape of an equilateral triangle. So, I switched to a different modeling approach. I found it preferable to model the three solid branches directly with 3-sided prismatic beams (Fig.5a), which are then connected to the two 3-sided pyramids that support the top and bottom vertices (Fig.5b). By recoloring the facets, I can identify the three ribbon-like surface areas (yellow, orange, magenta) (Fig.5c), and I can find out what edges have to be labeled as "sharp." To obtain the desired smooth surface (Fig.5d), the enhanced polyhedral model is subjected to three levels of Catmull-Clark subdivision [1] in which the sculptural sharp edges are prevented from being rounded in the subdivision process. This results in nice, smoothly shaped face strips, even when the starting polyhedral model is rather coarse. This model can then be converted into an STL-file and sent to a low-end 3D-printer [8]. The first model was printed in a dark filament, and its intriguing, curved, ribbon-like faces did not photograph well; therefore, I painted it in a bright yellow color (Fig.1e).

Actually, defining the sharp edges in these polyhedral models is somewhat challenging. Again, I want to exploit the symmetry of these objects, and I don't want to have to specify every single sharp edge in a hierarchically flat, polyhedral model. I want to define just one "ribbon country" (yellow in Fig.5c) and then use it two more times (shown in orange and magenta). Therefore, I must make sure that all the edges of the prototype ribbon face are marked as *sharp*. The four polylines marked in green, silver, black, and blue in Figures 2(a,b) achieve that goal. Figure 5d shows the result of smoothing the polyhedral model with three levels of CC-subdivision, and Figure 5e depicts the resulting shape with a proper set of *sharp* edges in the right places.

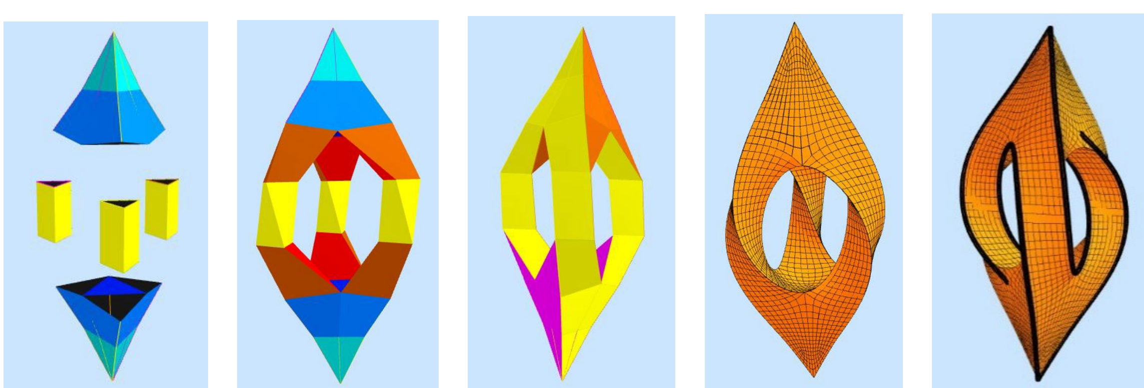

(a) (b) (c) (d) (e)

Figure 5: *Polyhedral modeling: (a) Placing pyramids and prisms; (b) components connected; (c) displaying the 3 ribbons countries; (d) after subdivision; (e) "sharp" edges enhanced.*

Derivative Sculptural Models with 3-Pass-Edges

In my paper for the 2024 Bridges Math-Art conference [5], I present several "derivative" models based on Tord's inspiring sculpture. In that first exploration, I increased the genus of the model by creating some "*E*-2-1"-geometries. In these models, all *E* edges start at the top vertex, move downwards past the central void, circle partially around two of the tunnels and then move downwards again to stop at the bottom vertex.

As the first derivative model, I created a "4-2-1"-handlebody. Its set of 4 loopy edges is shown in Figure 6a. However, I directly built a polyhedral model based on two 4-sided pyramids and four twisted, 3-sided prismatic legs (Fig.6b). Only one eighth of the new complex face of this sculpture needed to be constructed. The resulting polyhedral model (Fig.6c) can then be smoothed by Catmull-Clark-subdivision and turned into an STL-file that can be used to make a 3D-print (Fig.6d).

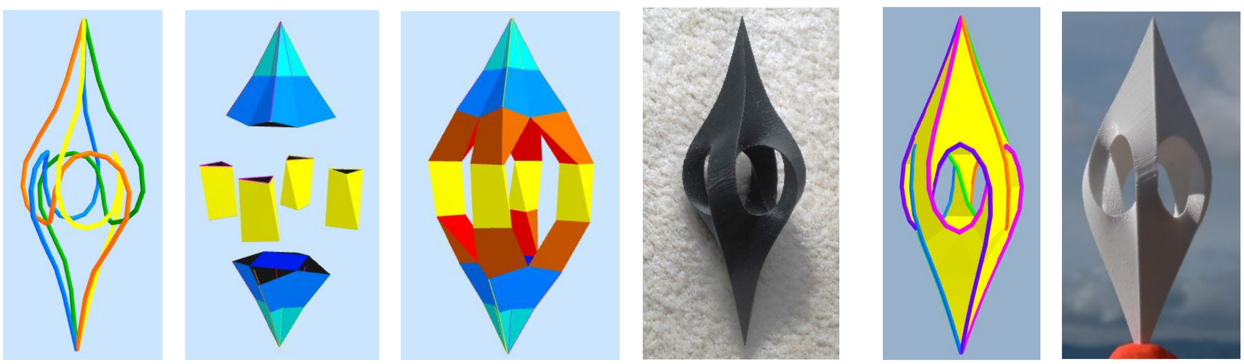

(a) (b) (c) (d) (e) (f)

Figure 6: *Increasing the rotational symmetry: (a) The 4 edges of a "4-2-1"-sculpture; (b) placing pyramids and prisms; (c) connecting the components; (d) 3D-print. (e) CAD model of a "5-2-1"-sculpture; (f) a 3D-print.*

The same approach also allowed me to make a "5-2-1"-sculpture (Figs.6e,f). It was not difficult to make these extended derivative shapes, since the behavior of all the edges in all the sculptures is always the same: Each edge starts at the top vertex, travels half-way down the sculpture, loops partially, counter-clockwise around one tunnel/window, travels along the inside of one of the prismatic branches, then partially loops clockwise around the adjacent tunnel/window, and then heads for the bottom vertex. To make the extensions shown in Figure 6, I just had to repeat this edge-behavior *E* times around the vertical rotational symmetry axis. The resulting surfaces can be understood as follows: There are *E* ribbon-like parts that run in a zig-zag manner from the upper *E*-way junction to the lower one. Each such ribbon starts at the internal junction patch and uses a first 3-sided prismatic branch to move to the outside, where it passes into one of the *E* lower pyramid faces. From that pyramid face, the ribbon travels through the outside of a branch to a top pyramid face. Then, on the other leg of that pyramid face, the ribbon moves again to the inside, where it joins the lower *E*-way junction. Given that all these ribbons connect to both the upper and lower *E*-way junctions, it is clear that all surface pieces connect into a single smooth "*face*" bordered by the *E* sharp edges.

New Explorations Using 5-Pass Edges

In all of the above models, the branches had a triangular cross-section, and all the loopy edges made three passes past the central void. Now I want to accommodate more complicated edge-curves on branches that have more than three prismatic sides. All sculptures will still have just two vertices, and all the edge-curves have identical shapes.

My initial goal was to construct a structure, where each edge passes once through each one of the five prismatic branches and gradually winds its way around the whole structure, as it does in Tengstrand's original “3-2-1”-sculpture (Fig.7a). This new “wiggly” edge would make 5 passes past the central void as it works its way once around the bi-pyramid structure. In Figure 7b, a single (green) edge winds through the five prismatic branches in the desired manner. In Figure 7c, a second (blue) edge has been added, rotated around the symmetry axis by 72 degrees. However, with this arrangement of edges, I was not able to find a set of five ribbon-like faces that could define a proper handlebody of genus 4. Suspending ribbon-like surfaces between neighboring edges always resulted in twisted facets that intersected with facets from neighbouring ribbons. And, when a third (orange) edge is introduced (Fig.7d), the edges themselves start to intersect.

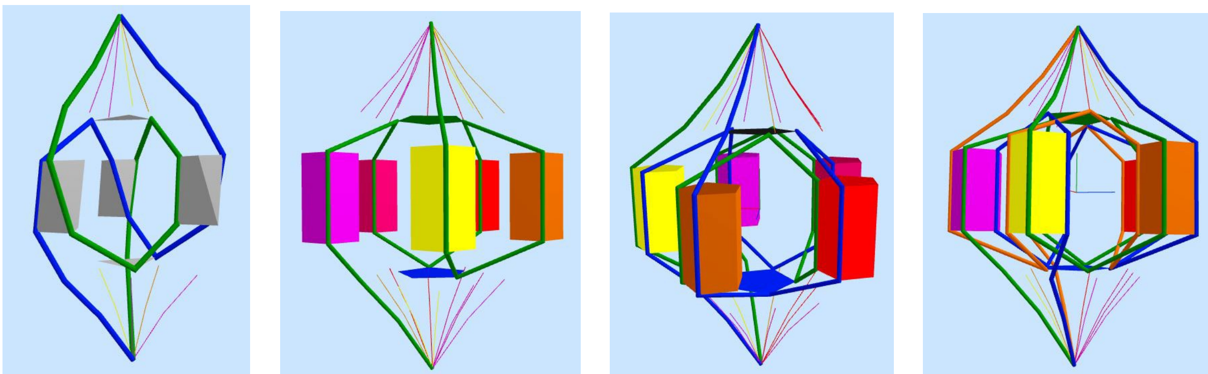

(a) (b) (c) (d)

Figure 7: *(a) Edge set-up of the original “3-2-1”-sculpture. (b) Similar edge setup for five pentagonal prism branches, with one edge highlighted; (c) a second such edge added; (d) three edges shown.*

On the other hand, I have been able to construct a good ribbon-face (yellow) that travels around just <u>two</u> adjacent tunnels. It starts at the upper 5-way junction, then passes through pyramid faces at both vertices (Fig.8a), and ends up at the lower 5-way junction. The ribbon travels three times along one prismatic branch, at the inside of which it runs adjacent to itself (Fig.8b); and it also runs once through both neighboring branches (Figs.8c). This then results in a 5-pass edge structure forming two loops (Figs.8d,e).

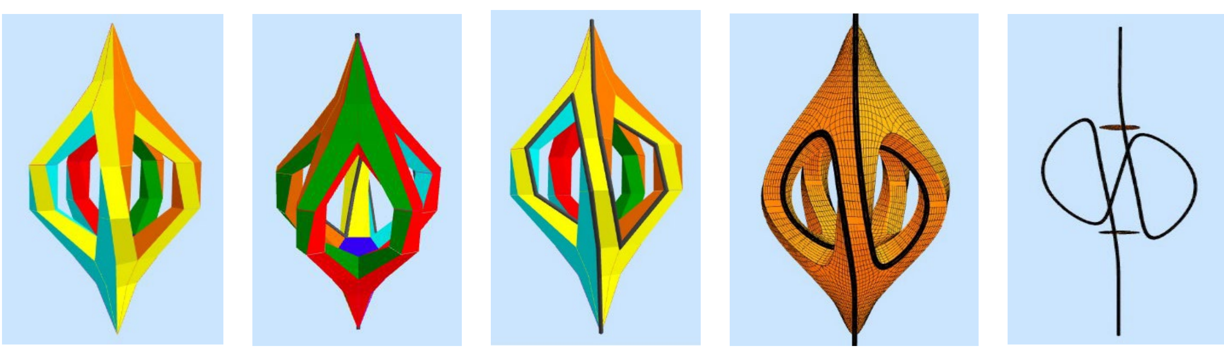

(a) (b) (c) (d) (e)

Figure 8: *A new type of a “5-2-1”-sculpture: (a) polyhedral model, (b) back-side view; (c) one edge highlighted. (d) after CC-subdivision; (e) extracted edge curve.*

This basic 5-pass, double-loop edge-shape can now be used in Tengstrand structures with a different number of prismatic branches, *B*. Figure 9 shows results for three, four, five, and six branches. In each case the 5-pass, double-loop edge-curves will be accommodated in three adjacent branches, as is also the case for the 3-pass edge-curve in the various enhanced Tengstrand sculptures shown in Figure 6. For *B*=*E*=3, this results in a new “3-2-1”-sculpture with a more complex edge shape (Figs.9a,b). There are always as many edges as there are branches in the handlebody (Figs.9c,d,e), and as long as all edges are of the 5-pass type, the branches are 5-sided prismtic beams.

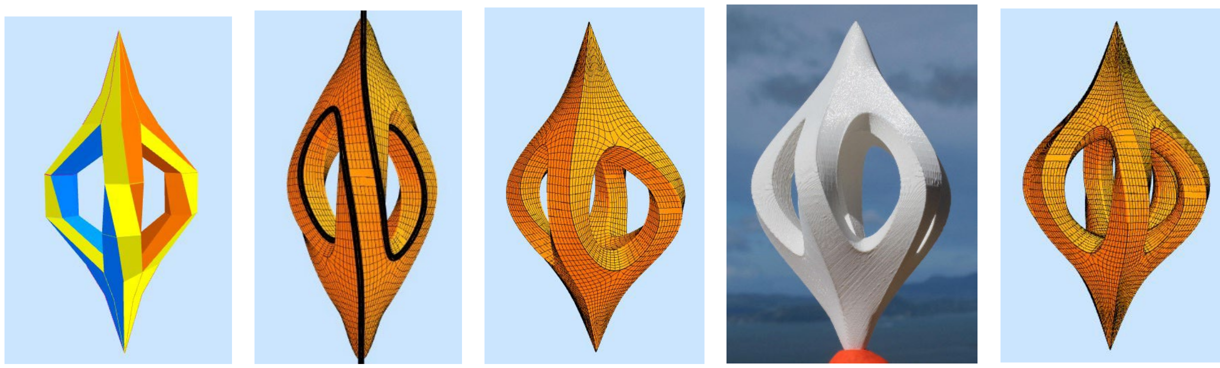

(a) (b) (c) (d) (e)

Figure 9: *Using 5-pass edges: (a) 3-branch "3-2-1"-polyhedral starting model; (b) model after 3-level CC-subdivision, with a single 5-pass edge highlighted; (c)"4-2-1"-CAD-model, (d) "5-2-1"-3D-print. (e)"6-2-1"-CAD-model.*

Derivative Tengstrand Structures with 4-Pass Edges

The reader may wonder why I jumped directly from the 3-pass edge structures that I explored in my Bridges paper to Tengstrand structures with *P*=5-pass edge curves, skipping over the case *P*=4. It turns out that when *P* is even, things get more complicated. *P*=4 implies that each edge makes <u>four</u> passes past the central void; and this means that an individual edge starting from the top vertex makes a "down-up-down-up" move and then ends up again at the starting vertex (Fig.10d). All edges now start and end on the same vertices! This leads to an additional constraint. To preserve the symmetry of these sculptures, the number of edges terminating at the top vertex should be same as at the bottom vertex. Overall the symmetry is reduced by a factor of 2, since in each pyramid corner there are now only *E*/2 edge-curves present.

Figure 10 shows a working edge configuration for *E*=*P*=4. In Figure 10a, just the two top edges are shown, while in Figure 10b all four edges are depicted. Each individual edge-loop passes twice through one of the four branches, and once each through each of the two neighboring branches. This then leads to a handlebody composed of four ribbon-shaped faces that show a similar behavior: They each run from one of the inner junction areas through the two pyramids and then back to their starting point, thereby forming some kind of a 4-pass loop (Fig.10f), brushing tangentially against the blue junction patch (Fig.10g). But the edge configuration described above seals off the 4-sided junction area on two opposite sides. While all four ribbon-loops approach the two (blue) 4-way junction areas, only <u>one</u> pair of ribbons can join in one junction area. The other two pass the junction tangentially, separated from it by a sharp edge (Figs.10h,i).

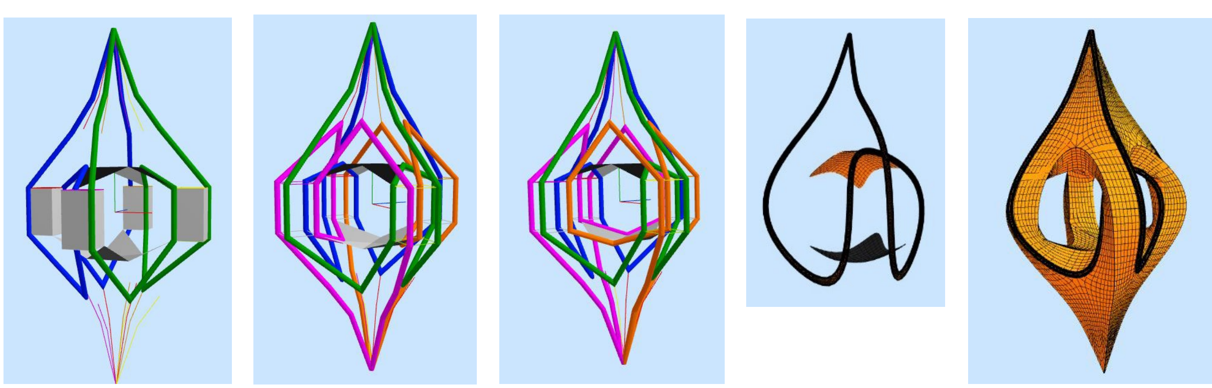

(a) (b) (c) (d) (e)

Figure 10: *(a) General set-up of a "4-2-(?)"-sculpture, showing the two edges hooked to the top vertex. (b) All four edges shown resulting in a "4-2-3"-structure. (c) Bottom two edges rotated by 90 degrees, resulting in a "4-2-2"-structure. (d) A single edge-loop smoothed. (e) Smoothed "4-2-2"-model.*

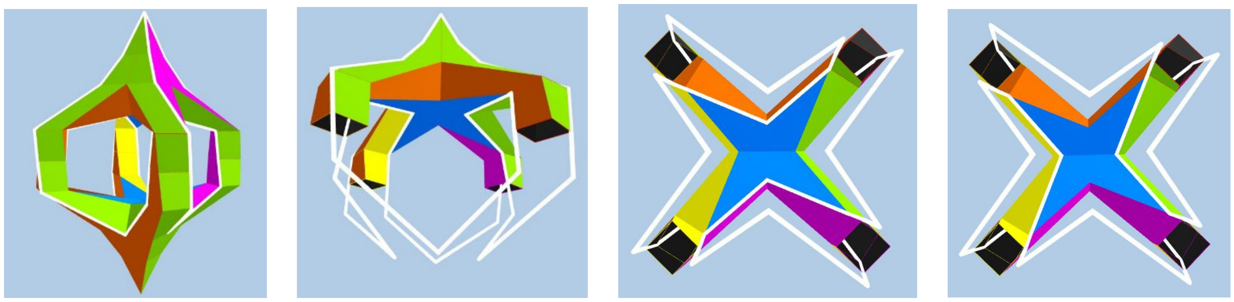

(f) (g) (h) (i)

Figure 10(ext.): *(f) Bi-pyramid frame with the two top 4-pass edges shown. (g) Inside view of top half, showing blue junction patch. (h) Edges placed to allow the yellow & lime ribbon loops to merge. (i) Edges rotated 90° allow the orange & magenta loops to merge through the blue patch.*

For the edge configuration shown in Figure 10b the same pair of ribbons will join in the top junction as well as in the lower one; this leaves two of the four ribbons isolated, and this results in a "4-2-3"-geometry. If the bottom two edges are rotated by 90 degrees (Fig.10c), one pair of ribbons merges in the top junction, and the other pair merges in the lower one; thus overall there are now only to *faces*, and the result is equivalent to a "4-2-2"-structure. Figure 10d depicts a single edge-loop smoothed with CC-subdivision; and Figure 10e shows this edge-loop in the context of the complete sculptural model.

Figure 11 shows pairs of topologically different sculptures. In Figure 11a I have painted the two merged *faces* in yellow and in green, respectively. When the bottom edge pair is rotated by 90 degrees, a "4-2-3"-structure results, since the red and the yellow ribbons are prevented from merging (Fig.11b).

Similarly, Figure 11c depicts a "6-2-2"-structure. If the three edge-curves hooked to the bottom vertex are rotated by 60 degrees, a "6-2-4"-structure results, because now three ribbons merge in both (white) 3-way junctions, while the other three ribbons remain isolated (Fig.11d).

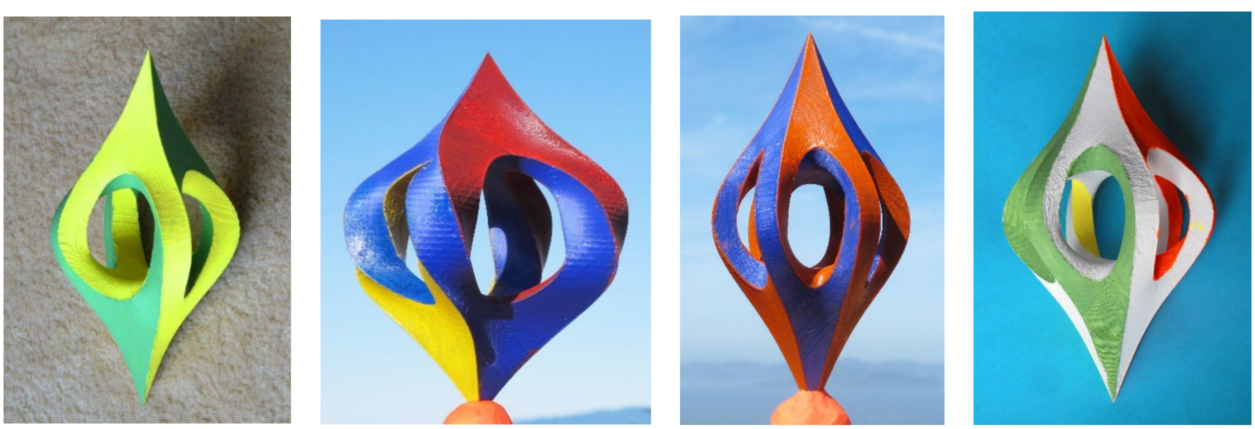

(a) (b) (c) (d)

Figure 11: *Painted models: (a)"4-2-2"shape; (b)"4-2-3"shape; (c)"6-2-2"shape; (d)"6-2-4"shape.*

Handle-Bodies of Genus-1 and "Arch" Modules

Somewhat surprisingly, the edge geometries and the behaviour of the "ribbon countries" discussed above can also be made to work on handlebodies of genus 1, with only two twisted prismatic branches between the two vertices. For the 3-pass edge-curve, this then results in a "2-2-1"-handlebody (Fig.12a).

When the two edges are joined at the tips of the two pyramids, we obtain a single curve that is topologically equivalent to a (2, 3)-torus-knot. For the more complicated *P*-pass edges with an odd *P*, the result is a (2, P)-torus-knot; for instance, the (2, 5)-torus-knot shown in Figure 12(b). For even values of P, we do not get the doubly covered (2, P)-torus-knot but two simpler (1, P/2)-torus-knots, which are out of phase by 180 degrees. Between them they accommodate two ribbon-like surface strips, shown in red and blue for P=4 (Fig.12c). We can contemplate what would happen if we used even simpler 2-pass edges: This would result in two interlinked (1,1)-Torus-knots. But this also implies that the two prismatic connecting branches are just 2-sided "prisms," i.e., flat ribbons (Fig.12d).

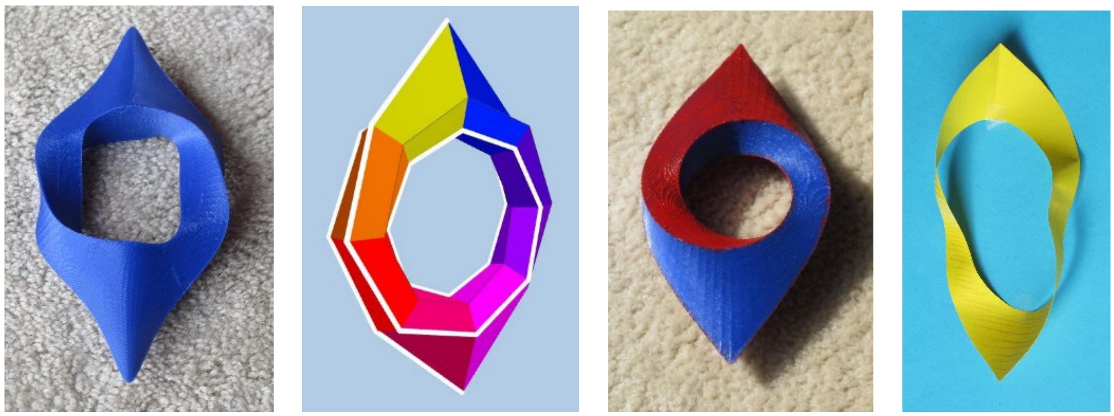

(a) (b) (c) (d)

Figure 12: *(a) "2-2-1"-structure leading to a (2, 3)-Torus-knot. (b) (2, 5)-Torus-knot. (c) 4-pass edges leading to two (1, 2)-Torus-knots. (d) Two linked (1, 1)-Torus-knots.*

The shapes presented in Figure 12 are of some modeling interest. I split them along the equatorial planes into two "arch"-like "half-modules" that form useful construction components (Fig.13a,d). An even number of these modules can be strung togther into an up-down zig-zag loop. Figure 13b displays a zig-zag loop with a square footprint built from four arch modules with legs with a triangular cross-section; this required a slight adjustment of the twisting of the two legs. It is more natural to fit six of these arches into a zig-zag ring with a hexagonal footprint (Fig.13c). On the other hand, four arches with square legs (Fig.13d) can readily be assembled into a ring with a square footprint (Fig.13e); it has been painted to show that this model has four individual ribbon-like faces.

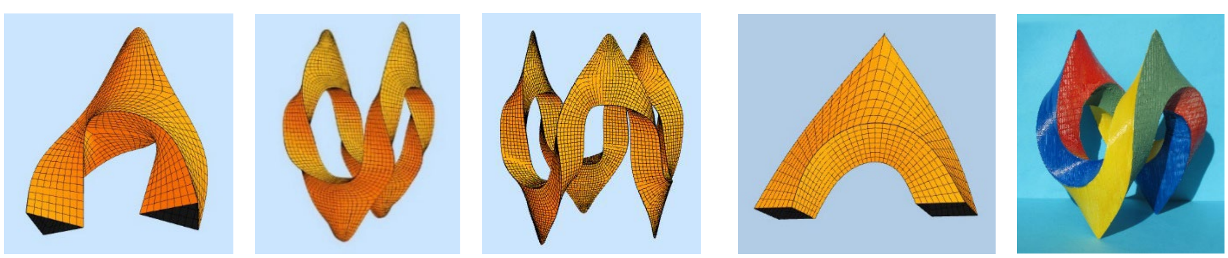

(a) (b) (c) (d) (e)

Figure 13: *(a) Half of Fig.12a. (b) Four such arches form a zig-zag structure with a square footprint. (c) 6-arch zig-zag structure with hexagonal footprint. (d) Half of Fig.12c. (e) 4-arch zig-zag ring.*

Combining "Legged-Pyramid" Half-Modules

The above constructions prompted me to also split the higher-genus structures into pairs of B-sided pyramidal "half"-modules with B legs, and then connect these modules into more complicated frame structures based on the Platonic polyhedra. Figute 14 shows the example of a half-module derived from the original Tengstrand sculpture with 3-pass edges on a handlebody with 3 branches (Fig.5b). I wanted to place four such modules at the corners of a tetrahedron and join their legs.

In order to obtain flush connections between the legs of neighboring "half"-modules, I introduced additional geometrical parameters into th three legs. I made the triangular prisms at the end of each leg adjustable in diameter, azimuth, and twist, and I added the freedom to adjust the tilt and the separation of these prisms to spread the three legs of the pyramid more broadly (Fig.14b). It was not surprising that four such "half-modules could be assembled into a tetrahedral frame (Fig.14c), and that, with the right edges marked as *sharp* (Fig.14b), the whole frame can be CC-subdivided [1], and the sharp edges would appear in the right places (Fig.14d).

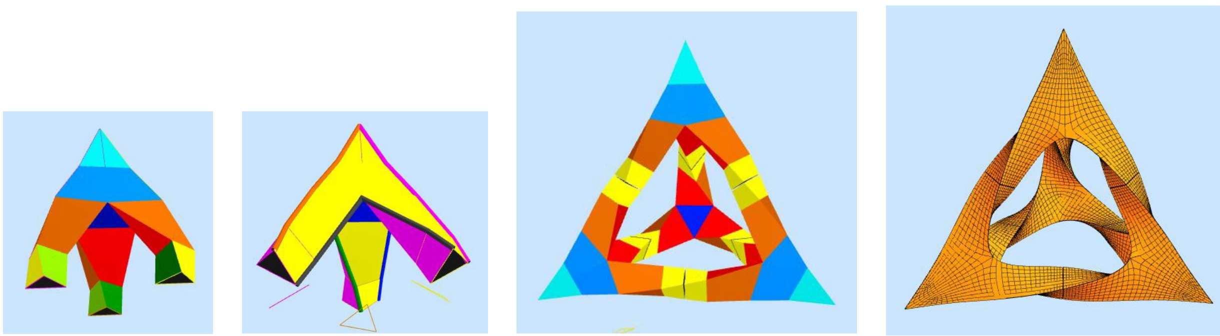

(a) (b) (c) (d)

Figure 14: *(a) Half of Figure 5b. (b) "Half"-module with "flexible" legs and specified sharp edges. (c) Tetrahedral assembly of four "half"-modules; (d) after CC-subdivision with sharp edges.*

A remaining question was: What kind of edge-pattern would emerge in the overall tetrahedral structure? It turns out that there are just six separate, smooth, "loopy" edge curves. Each one follows a contorted path that starts at one pyramid vertex, passes on the inside of two other corner pyramids, and then ends on the fourth vertex (Fig.15a). I would not have been able to design directly such a path based on a B-spline. It is interesting to note that the 3-pass edge in the bi-pyramid handlebodies turns into a "3-segment" sharp edge on the tetrahedral frame.

A similar question concerns the ribbon-like portions of the resulting single "face." There are six separate ribbon countries. They start at one internal 3-way junction patch, pass through two pyramid faces, and then end at the junction inside the fourth pyramid. Figure 15b shows one such ribbon country painted on the tetrahedral frame. Six of those placed properly at the six edges of the tetrahedron completely cover the underlying handlebody (Fig.15c). However, all six ribbons are smoothly connected to one another through the four inner (black) junction areas, so that they form a single Tengstrand-style *face*.

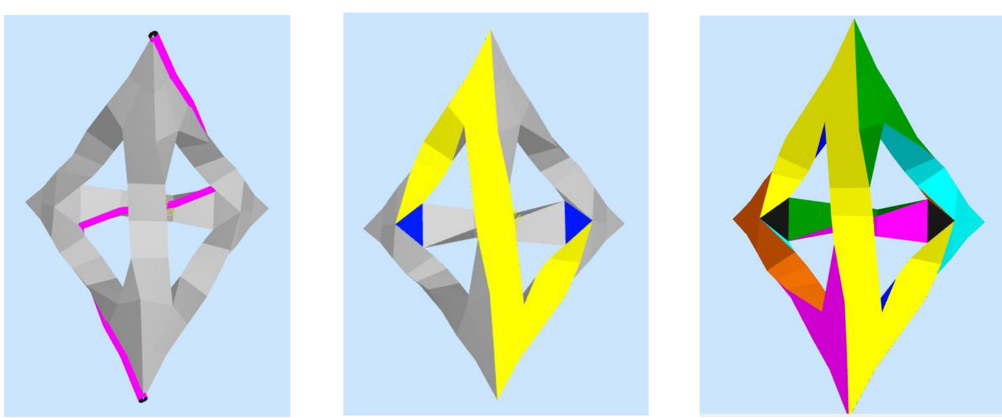

(a) (b) (c)

Figure 15: *Tetrahedra with: (a) one 3-segment edge. (b) one 3-segment ribbon. (c) six ribbons.*

In the same spirit, a somewhat differently deformed 3-legged corner pyramid can be used to construct a cuboidal frame (Fig.16a). Here we find twelve edges (Fig.16b) and twelve ribbon countries with a behavior similar to that in the tetrahedral frame. However, as a special case for the cuboidal frame, a single half-module using three colors, and its mirror image can be assembled in a way that produces a consistent coloring with only three colors for all twelve ribbon areas (Fig.16c). This is because among all five Platonic polyhedra, only in the cube can the two types of vertices (mirrored and non-mirrored) be placed in such a way that the two neighbors across any leg-joints are always of different types.

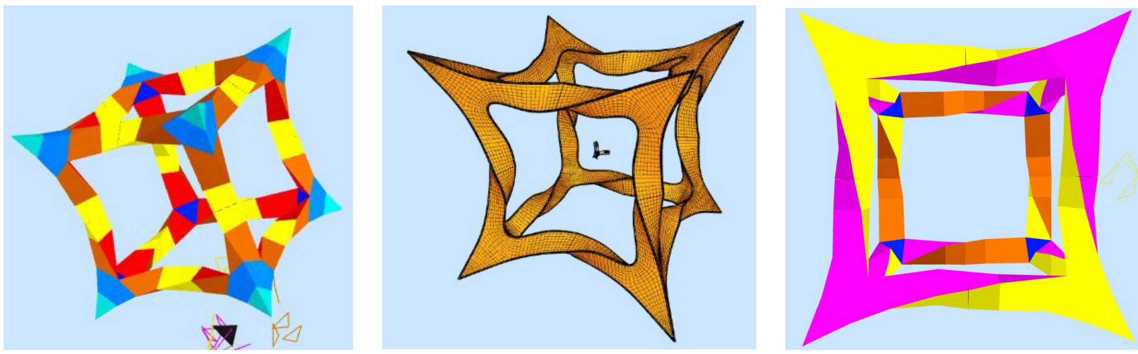

(a) (b) (c)

Figure 16: *(a) Cuboidal frame. (b) Twelve 3-segment edge-curves stretching from vertex to vertex. (c) Twelve surface ribbons painted with only three colors.*

For the construction of an octagonal frame (Fig.17d,e), we need six valence-4 pyramid half-modules with four legs. A polyhedral starting module (Fig.17a) can readily be obtained by splitting Figure 6c along the equatorial plane. Its legs are then spread to accommodate an octahedral frame (Fig.17b) and its edges are marked with appropriate sharp specifications (Fig.17c). The assembly of six half-modules (Fig.17d) is then subdivided and converted into an STL-file to fabricate a 3D-print (Fig.17e).

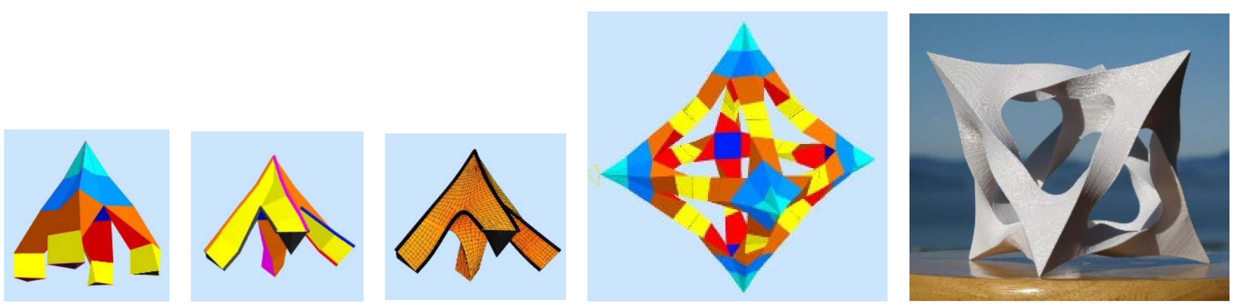

(a) (b) (c) (d) (e)

Figure 17: *(a,b,c) Valence-4 pyramid corner modules. (d) Six pyramid-modules assembled into an octahedral frame. (e) 3D-print of the octahedral assembly.*

Figure 18 shows the equivalent constructionof an icosahedral frame using twelve valence-5 pyramid corner modules. When trying to make a 3D-print of this rather dense frame structure (Fig.18b) on an inexpensive printer [8], one encounters the problem of having to remove a large amount of support material trapped in the interior of the frame. It is thus advantageous to to print this object in two parts (Fig.18c); this requires less support, and the support material is easier to remove. The two half-parts can then be glued together.

In the same way one can readily build a dodecahedral model by assembling twenty 3-legged corner modules.

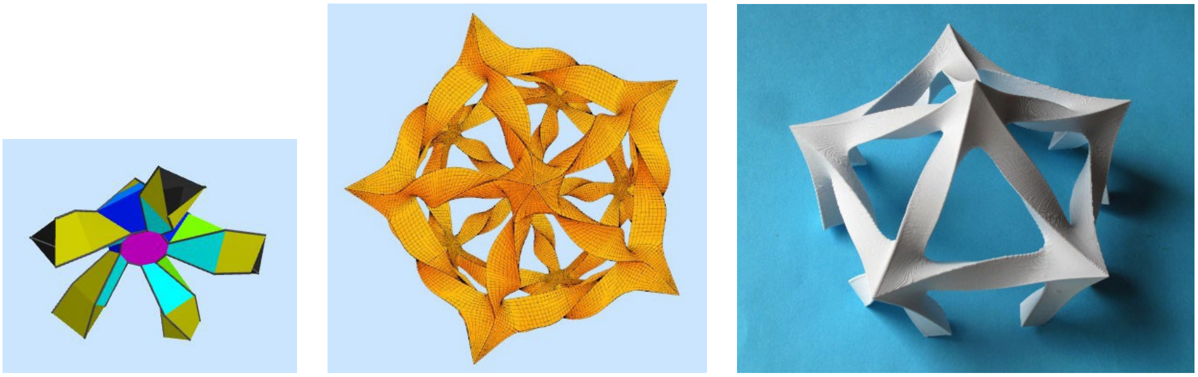

(a) (b) (c)

Figure 18: *(a) Valence-5 pyramid corner module. (b) Twelve pyramid modules assembled into an icosahedral frame. (c) 3D-print of half of an icosahedral frame.*

Platonic Frames with 4-Pass Edge-Curves

All five Platonic frames can readily be constructed with corner-modules based on 3-pass edges. A more interesting investigation is to look at half-modules derived from more complicated *P*-pass edge-curves; in particular the ones with an even value of *P*.

Let's take a close look at an octahedral frame based on a 4-pass edge-curve. I started by splitting Figure 11(b) into two half-modules (Fig.19a) and combining two of those into a bi-pyramid structure (Figs.19b,c,d). On this structure I study the behavior of the four 4-pass edges and the emerging ribbon-like surface elements. As shown in Figures 11(a) and 11(b), depending on which ribbons are allowed to merge in one of the two junction areas, the handle-body might be covered with either two (Fig.19b) or three (Fig.19c) separated *faces*. I now use the upper half of either one of these two structures as a 4-leg pyramid module to construct an octahedral frame composed of six such modules; I spread the four legs and adjust their tilt angle to 45 degrees (Fig.19e) to result in smooth leg-joints. Unfortunately, assembling six such modules does not automatically lead to contiguously colored ribbon segments; and even by rotating individual modules through steps of 90 degrees I could not produce a consistent, contiguous coloring. Similar to the problems discussed for the tetrahedral frame, the reason is that the legs of three modules forming a triangular cycle have an odd number of binary color changes and we always end up with one leg-joint with mismatched colors. The 4-pass edges do not solve this problem either.

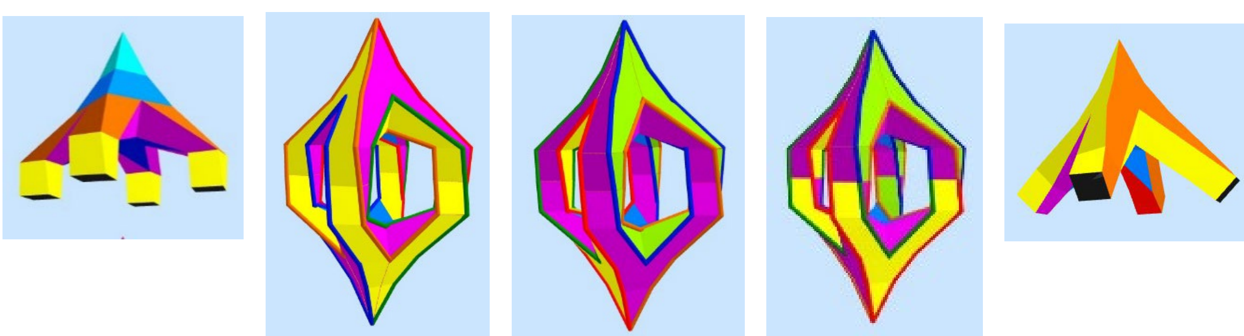

(a) (b) (c) (d) (e)

Figure 19: *(a) Half of Fig.11b. (b) 2-color bi-pyramid. (c) 3-color bi-pyramid, (d) lower half turned 90°. (e) Half-module adjusted to serve as a corner of an octahedral frame.*

However, I was still able to extract the general behaviors of the edges and ribbons in an octahedral frame built from these pyramid modules: Similar to Figure 15(a), each edge starts at the outer tip of a pyramid module, but it now consecutively passes on the inside of <u>three</u> further modules, and then ends up at the tip of another pyramid module. This can be considered some kind of a "4-pass" move; and I will call this a "4-segment" edge. Figure 20a depicts five such 4-segment edges drawn on the polyhedral octa-frame. The red edge is rotated around the *z*-axis (perpendicular to the image plane) in steps of 90 degrees to generate the other three edges starting from the front (blue) vertex; and it is rotated 90 degrees around the *x*-axis to produce the dark blue instance of the 4-segment edge. In total, there are twelve such edges.

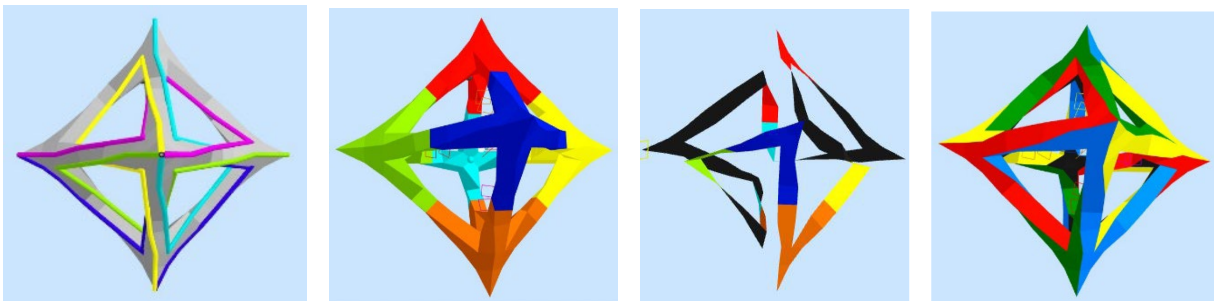

(a) (b) (c) (d)

Figure 20: *(a) Octa-frame with five 4-segment edges highlighted. (b) Color-coded pyramid-modules. (c) 12-segment ribbon-loop passing twice through every corner. (d) 4 loops form an octa-frame.*

The ribbons follow a more complicated pattern. Without the use of any mergers through any (black) junction patch, the ribbon areas form four 12-segment loops. In Figure 20b, I have colored the six pyramid modules differently to keep track of the travel of an individual ribbon loop (Fig.20c). The loop passes through every pyramid-module twice. It makes two consecutive inner passes that lead directly from one junction patch to another one. Then it passes through two outer pyramid faces, where it makes sharp hairpin turns before it tangentially touches another junction patch. This pattern repeats three times to complete the 12-segment loop. Four such ribbon loops assemble into a complete octa-frame (minus the six black junction patches) (Fig.20d).

Thus, before the role of the junction patches is considered, the total number of smoothly connected faces is already reduced to 4. In addition, at every junction patch one pair of ribbon-loops that touch the junction patch on opposite sides will merge through that junction patch, while the other two opposing loops remain isolated from the junction patch by two sharp edge segments.

As individual pyramid-modules get rotated in 90-degree steps, the pattern of the ribbon faces remains the same, but the connectivity between the four 12-segment loops changes. When I chose the original rotations to put the six pyramid-modules at the vertices of an octahedron, I treated them as if they had full 4-fold symmetry, and I paid no attention to their locally reduced symmetries due to the junction patches that are bordered on two of their four sides by sharp edges. Further investigation is required to find out what combinations of these six independent rotation parameters will lead to an overall octahedral frame with the highest degree of symmetry. However, every color combination appears at least once in one of the six junction areas, so this should make it possible to merge all four loops into a single, smoothly connected *face*. This would then result in a "12-6-1"-Tengstrand structure.

Summary

In Tengstrand's original "3-2-1"-sculpture, three identical *edges* wind around the three *branches* connecting the two *vertices* in a 3-sided by-pyramidal frame structure. These three edges delineate only one single, complex, smoothly connected "*face*," embedded in the surface of a genus-2 handlebody. My exploration started with an investigation of what happens when the number of edges, *E*, is changed from *3* to another small integer number, *E*. In the first derivative designs, I maintained *E*-fold rotational symmetry around an axis that connects the two vertices, and I also maintained the *E* connecting branches as 3-sided, twisted prismatic rods (Fig.6). This generalization was rather straightforward, and it always resulted in a handlebody of genus (*E*–1) with a single *face* covering the whole surface.

I subsequently studied what happens when I use more complicated edge-curves that make more than three passes past the central void in the bi-pyramid. To accommodate *P*-pass edges (and *ribbons*) I also increased the number of polygonal sides in the prismatic branches to *P*. Now *P* edges and *P* ribbon segments pass through every branch (Fig.9). When *P* is an <u>even</u> number, the situation becomes more complicated. The resulting edges then start and end at the same vertex. This constrains the number of edges, *E*, to be even; and this reduces the resulting symmetry of the resulting sculpture by a factor of two. Moreover, depending on how I arranged the edge-loops hooked to the two corner pyramids with respect to one another, the number of resulting *faces* could be changed, but the <u>minimum</u> number of faces was always two (Fig.11).

I also used <u>half</u> of these bi-pyramidal frames as pliable *half-modules* to generate more complex symmetrical frame structures. In all the resulting handlebodies, I kept all the edges and all the corner structures exactly the same. When *E* was set to *2*, I could connect several of these *arch*-shaped half-modules into closed-loop chains of genus-1. For instance, six such modules can be connected into a zig-zag structure with a hexagonal footprint (Fig.13c). The pyramid corners with more than two legs were also used to construct highly symmetrical frames based on the Platonic polyhedra (Figs.14-18).

The structures analyzed and discussed in this paper have two key parameters, *E* and *P*, specifying the number, *E*, of *sharp*, *P*-pass edges. The number of physical, prismatic branches, *B*, is always the same as the number of sharp edges, and the number of polygonal sides in these branches is equal to *P*, accommodating the *P* "segments" of the zig-zag-shaped edge curves. Similarly, the resulting 2D surfaces of these physical objects are composed of *E* zig-zag-shaped *P*-segment *ribbons*, which are connected to some degree in the *V* junction areas below the *pyramid* corners of the overall frame structure. This is true for the simple bi-pyramid structures as well as for the Platonic frames.

Conclusions

Tengstrand's "*edges-vertices-faces*"-notation is primarily a topological characterization of bi-pyramid handlebodies covered with a mesh of sharp edges. In choosing specific geometries to introduce my new derivative models, I designed shapes that could depict the 3D results easily through 2D images, and which also stayed true to the "character" of the original Tengstrand sculpture.

To decide whether a new handlebody still belonged into the *Tengstrand Family*, my primary criterion was whether all the edge-curves had the same shape. This criterion readily includes all the bi-pyramid designs and the Platonic frame structures. The issue became more intricate when I started to explore some Archimedean frames. Most of these frames clearly fall <u>outside</u> the boundaries of the *Tengstrand Family*, because not all the edges have the same pair of neighboring faces.

But the cuboctahedron (Fig.21a) and the icosidodecahedron are exceptions; here all edges and vertices are the same. However, the corner modules no longer have 4-fold rotational symmetry; they assume a more rectangular pyramid shape with only 2-fold rotational symmetry. For 3-pass edges this is good enough to give all edge-curves the same shape (Fig.21b) and keep this frame in the *Tengstrand Family*.

A more daring move is to look at the <u>duals</u> of these two Archimedean polyhedra. They both comprise two different types of vertices with valences 3 & 4, and 3 & 5, respectively; and this might already put them outside the bounds of the *Tengstrand Family*. On the other hand, on the rhombic dodecahedron (Fig.21c), every 3-segment edge-curve starts on one type of vertex (valence 3) and ends on the second type (valence 4), thus the edges can still be all the same. The same is true for the 3-segment ribbon structures. Thus, a rhombic-dodecahedral frame with twisted prismatic edges can still be considered to lie in the *Tengstrand Family*.

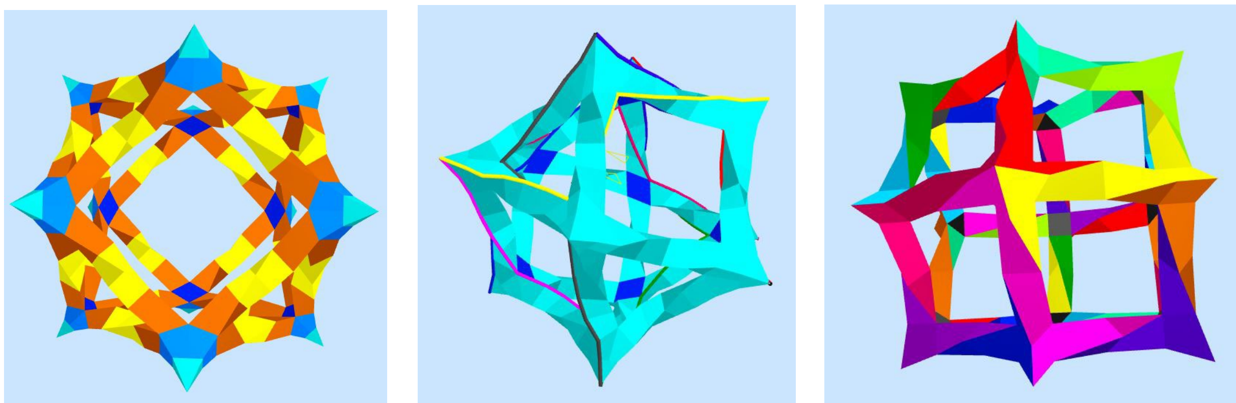

(a) (b) (c)

Figure 21: *(a) 3-pass cuboctahedron; (b) overlaid with ten colored copies of a 3-pass edge-curve. Rhombic dodecahedron painted in 12 different colors to show the 24 3-segment ribbon countries.*

In summary, joining twisted prismatic beams in symmetrical configurations can lead to intriguing geometrical shapes. I am still surprised that the original, inspiring sculpture by Tord Tengstrand has led to so many different shapes and presented me with many puzzles and design challenges.

Acknowledgment

I am grateful to Tord Tengstrand for presenting his "3-2-1"-sculpture at Bridges 2020, and for involving me in a lively email discussion about its geometry and its topology. This allowed me to do the fascinating exploration presented in this paper.

References

[1] E. Catmull, J. Clark. "Recursively generated B-spline surfaces on arbitrary topological meshes." – https://people.eecs.berkeley.edu/~sequin/CS284/PAPERS/CatmullClark_SDSurf.pdf

[2] G. Dieppedalle. "Interactive CAD Software for the Design of 2-manifold Free-form Surfaces." Tech-Report (EECS-2018-48). – https://www2.eecs.berkeley.edu/Pubs/TechRpts/2018/EECS-2018-48.pdf

[3] R. Fan, C. H. Séquin, R. Ng. "Joining Interactive Graphics and Procedural Modeling for Precise Free-Form Designs." Tech-Report (EECS-2021-125) May 14, 2021. – https://www2.eecs.berkeley.edu/Pubs/TechRpts/2021/EECS-2021-125.html

[4] JIPCAD Language Reference. – https://tinyurl.com/9ds62ee2

[5] C. H. Séquin. "Handle-Bodies Inspired by Tengstrand's "3-2-1"-Sculpture." Accepted for Bridges 2024.

[6] J. Smith. "SLIDE design environment." (2003). – https://people.eecs.berkeley.edu/~ug/slide/

[7] Tord Tengstrand "3-2-1-Sculpture." Bridges 2020 Art Exhibit – https://gallery.bridgesmathart.org/exhibitions/2020-bridges-conference/tordtengstrandteliacom

[8] Ultimaker. "Reliable 3D printers." – https://ultimaker.com/3d-printers